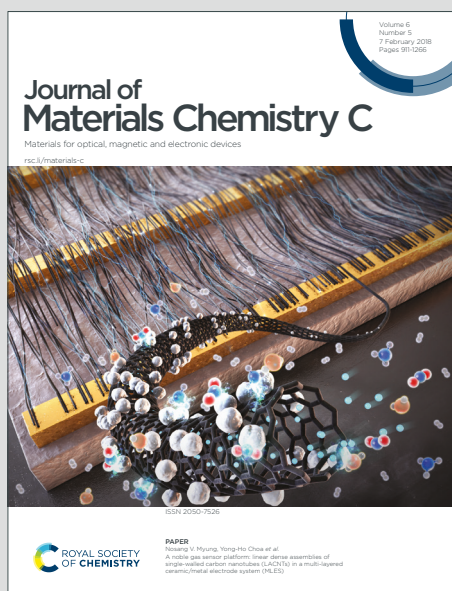


Journal of Materials Chemistry C

Materials for optical, magnetic and electronic devices

Accepted Manuscript

This article can be cited before page numbers have been issued, to do this please use: N. Sun, K. Su, Z. Zhou, X. Tian, D. Wang, N. Vilbrandt, A. Fery, F. Lissel, X. Zhao and C. Chen, *J. Mater. Chem. C*, 2019, DOI: 10.1039/C9TC02001B.



This is an Accepted Manuscript, which has been through the Royal Society of Chemistry peer review process and has been accepted for publication.

Accepted Manuscripts are published online shortly after acceptance, before technical editing, formatting and proof reading. Using this free service, authors can make their results available to the community, in citable form, before we publish the edited article. We will replace this Accepted Manuscript with the edited and formatted Advance Article as soon as it is available.

You can find more information about Accepted Manuscripts in the [Information for Authors](#).

Please note that technical editing may introduce minor changes to the text and/or graphics, which may alter content. The journal's standard [Terms & Conditions](#) and the [Ethical guidelines](#) still apply. In no event shall the Royal Society of Chemistry be held responsible for any errors or omissions in this Accepted Manuscript or any consequences arising from the use of any information it contains.

Synergistic effect between electroactive tetraphenyl-*p*-phenylenediamine and AIE-active tetraphenylethylene for highly integrated electrochromic/electrofluorochromic performances

Received 00th January 20xx,
Accepted 00th January 20xx

DOI: 10.1039/x0xx00000x

www.rsc.org/

Ningwei Sun,^{‡a,b} Kaixin Su,^{‡a} Ziwei Zhou,^b Xuzhou Tian,^a Daming Wang,^a Nicole Vilbrandt,^b Andreas Fery,^b Franziska Lissel,^{*b} Xiaogang Zhao^{*a} and Chunhai Chen^{*a}

Switchable fluorescent materials have gained great attention due to their promising applications in sensors, memory devices and displays. However, further progress is hindered by the low fluorescence contrast, modest response speed and inferior long-term cycling stability. Based on a rational design strategy by combining a highly conjugated tetraphenyl-*p*-phenylenediamine (TPPA) unit and an aggregation induced emission (AIE)-active tetraphenylethylene (TPE) unit, we synthesized a novel diamine “*N,N'*-bis(4-aminophenyl)-*N,N'*-di(4-(1,2,2-triphenylethenyl)phenyl)-1,4-phenylenediamine” to construct an electro- and AIE-active polymer. In addition to the high efficiency solid-state fluorescence and the extremely stable redox properties, the resulting polymer TPE-TPPA-PA realized highly integrated emission/color dual-switchable properties, including multistage color-changing, high fluorescence on/off contrast up to 252, impressively rapid response rate (1.3/0.5 s for EC and 0.7/2.1 s for EFC processes) and excellent cycling stability over 10000 s. The demonstrated synergistic effect between stable electroactive TPPA and AIE-active TPE may provide a new pathway for further molecular design to realize high-performance emission/color dual-switchable materials.

Introduction

Unlike most mammals, humans are primarily guided by our visual sense, driving research into innovative stimuli-responsive optical materials.¹⁻⁵ Among these, electrofluorochromic (EFC) materials, allowing a controllable fluorescence modulation by electric stimulus, possess vast prospects for applications in sensors, information encryption and displays.⁶⁻⁸ In general, EFC materials can be classified into three categories: electroactive/fluorescent composites, molecular fluorophores and intrinsically switchable fluorescent polymers.⁹⁻¹⁴ Compared with the other two types, intrinsically switchable fluorescent polymers are deemed as more promising candidates owing to their facile structural tunability, fast response speed and competitive processability. To date, only a few EFC polymers have been exploited. E. Kim et al. described the electrochemical fluorescence switching of photo-patternable polyoxadiazole, which exhibited a reversible fluorescence switching over 1000 cycles but only with a low fluorescence on/off contrast of 2.5.¹⁵ Poly(4-cyanotriphenylamine) reported by Liou et al. made a breakthrough for EFC polymers as it showed high fluorescence

contrast up to 242 with a rapid response time of 0.4 s/38 s. However, the high oxidation potential (1.25 V) caused by the introduction of the electron-withdrawing cyano group could decrease the electrochemical and EFC stability.¹⁶ Despite great efforts devoted to the design of novel EFC polymers, to the best of our knowledge, few of them could simultaneously comprise all the features needed for high-performance EFC materials, namely high fluorescence on/off contrast, fast response speed and excellent long-term cycling durability. Therefore, a further molecular-design guided optimization to enable the preparation of more sophisticated electroactive/fluorescent polymers is in great demand to realize highly integrated EFC performances.

Among the key EFC parameters, especially the high on/off contrast is essential. However, most EFC materials reveal low contrast ratios due to a weak fluorescence in the solid state, resulting from the aggregation-caused quenching of conventional luminophores.^{17,18} To circumvent this drawback, the introduction of aggregation-induced emission (AIE)-active luminophores is a facile and effective method to obtain materials exhibiting a higher fluorescence when utilized as solid films. Tetraphenylethylene (TPE) with four peripheral phenyl rings is a prototypical AIE-active luminogen and has been intensively investigated by Tang and coworkers.¹⁹⁻²⁴ In dilute solution, the isolated TPE molecules emit no fluorescence. Upon aggregation formed in the solid state, TPE derivatives are found to possess efficient light emission attributed to the mechanism of restricted intramolecular rotation (RIR). Although TPE is redox active, its high oxidation potentials and poor reversibility severely restrict its applications in EFC devices.²⁵ Consequently, exploring a

^a Key Laboratory of High Performance Plastics (Jilin University), Ministry of Education, National & Local Joint Engineering Laboratory for Synthesis Technology of High Performance Polymer, College of Chemistry, Jilin University, Changchun 130012, PR China

^b Leibniz Institut für Polymerforschung Dresden e.V., Hohe Str. 6, D-01069, Dresden, Germany

† Electronic Supplementary Information (ESI) available. See DOI: 10.1039/x0xx00000x

‡ N. Sun and K. Su contributed equally to this work.

novel molecular-design strategy by combination of TPE and electroactive moieties with low trigger potentials is of great significance. Triphenylamine (TPA) with its star-shape structure is well known for the photoactive and electroactive properties, which has been widely applied in light emitters, dye-sensitized solar cells, resistive memory and electrochromic (EC) devices.²⁶⁻³⁷ Recently, electroactive fluorophores with TPA and TPE moieties have been reported for EFC applications, effectively increasing the fluorescence on/off contrast.³⁸⁻⁴⁰ However, switching stability and response time, two important parameters for EFC materials, were not well realized due to the short conjugation and moderate stability of mono-TPA. Notably, TPA derivatives with extended conjugation, such as tetraphenyl-*p*-phenylenediamine (TPPA), usually possess improved HOMO levels and thus lowered oxidation potential. TPPA-based polymers revealed much enhanced electrochemistry and electrochromic switching stability even up to 10000 continuous cycles.⁴¹⁻⁴⁴ Furthermore, the highly twisty structures of TPE and TPPA can efficiently prevent the close packing of the polymer chains to thus accelerate the electrolyte ion transport.⁴⁵ And the highly conjugated TPPA can also enhance the intra-molecular charge mobility ability, potentially shortening the response time as well. Therefore, the design and construction of an electroactive fluorophore by combining TPPA and TPE moieties and incorporating it into polymer backbone is expected to synergistically improve the EC as well as EFC performances of the resulting polymers, surely promoting their commercial optical applications in the near future.

To show the promise of this design concept, in this study we carefully devised and synthesized a novel electroactive/AIE-active diamine, *N,N'*-bis(4-aminophenyl)-*N,N'*-di(4-(1,2,2-triphenylethenyl)phenyl)-1,4-phenylenediamine, as well as the derived semi-aromatic polymer (aliphatic structure leads to a reduced charge transfer effect, which will greatly increase the fluorescence¹⁷). By composing the electroactive luminophores to contain TPPA and TPE units, the resulting EC/EFC polymer is expected to highly integrate comprehensive performances including AIE effect, outstanding electrochemistry stability, high contrast ratio, fast responsive speed, superior cycling life and facile solution-processability. The careful design concept of the electroactive/AIE-active polymer is illustrated in Fig. 1, and its properties including solubility, thermal stability, electrochemistry, fluorescence, EC and EFC switching were studied in detail.

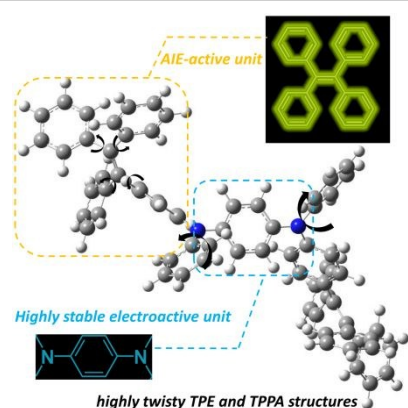


Fig. 1 Design concept of a high-performance EC/EFC polymer containing TPPA and TPE moieties. DOI: 10.1039/C9TC02001B

Experimental

Materials

Benzophenone (TCI), 4-bromobenzophenone (TCI), *p*-phenylenediamine (TCI), 4-fluoronitrobenzene (Acros), trimethylamine (Aladdin), TiCl₄ (Aladdin), zinc (Zn, TCI), potassium carbonate (K₂CO₃, Aladdin), copper powder (Aladdin), 10% palladium on charcoal (Pd/C, TCI), hydrazine monohydrate (TCI) and triphenyl phosphite (TPP, TCI) were used as received. Commercially available 1,4-cyclohexanedicarboxylic acid (CHDA, TCI) was dried under vacuum at 100 °C prior to use. *N*-methyl-2-pyrrolidone (NMP), dimethyl sulfoxide (DMSO), *o*-dichlorobenzene and pyridine (Aladdin) were dried using 4 Å molecular sieves prior to use. Tetrabutylammonium perchlorate (TBAP, Aladdin) was recrystallized twice from ethanol under nitrogen atmosphere and dried under vacuum prior to use. All the other reagents and solvents were used as received from commercial sources.

Monomer synthesis

1-bromo-4-(1,2,2-triphenylethenyl)benzene (TPE-Br, 1)

TPE-Br was synthesized through the McMurry reaction.⁴⁶ Zn powder (15.0 g, 231.3 mmol) was added to anhydrous THF (650 mL) in a three-necked round bottom flask under argon atmosphere. The resulting suspension was cooled to -5 °C, and TiCl₄ (12.7 mL, 115.6 mmol) was slowly added with a syringe. Then the above mixture was heated to reflux temperature for 3 h. Subsequently, the mixture was cooled to -5 °C again, charged with pyridine (7.5 mL), and stirred for another 0.5 h. Then a solution of benzophenone (7.5 g, 41.1 mmol) and 4-bromobenzophenone (8.6 g, 33.1 mmol) in 50 mL of THF was added into the mixture slowly, and the reaction proceeded for another 12 h at the reflux temperature. After the end of reaction (as monitored by TLC), the reaction was quenched by adding 10% K₂CO₃ aqueous solution and extracted with dichloromethane. The organic layer was collected and purified by chromatography using ethyl acetate/petroleum ether mixture (1:4) to get the desired product (7.6 g, yield 55%). ¹H NMR (300 MHz, DMSO-*d*₆, δ, ppm): 7.34 (d, *J* = 8.4 Hz, 2H), 7.22 – 7.09 (m, 9H), 6.98 (m, 6H), 6.90 (d, *J* = 8.4 Hz, 2H).

N,N'-di(4-nitrophenyl)-1,4-phenylenediamine (TPPA-2NO₂, 2)

TPPA-2NO₂ was synthesized according to a reported method with some modifications.⁴⁷ In a 500 mL three-neck round-bottom flask, a mixture of *p*-phenylenediamine (10.8 g, 100 mmol), 4-fluoronitrobenzene (32.4 g, 230 mmol), triethylamine (23.4 g, 230 mmol) and anhydrous DMSO (150 mL) was heated at 95 °C for 120 h. After cooling to room temperature, the mixture was poured into ice water, affording a mass of red powder. Then the crude product was purified by recrystallization for three times (DMSO/ethanol = 1:2) to give 11.2 g of red crystals (32 % of yield). ¹H NMR (300 MHz, DMSO-

d_6 , δ , ppm): 9.31 (s, 2H), 8.09 (d, $J = 9.3$ Hz, 4H), 7.27 (s, 4H), 7.03 (d, $J = 9.3$ Hz, 4H).

***N,N'*-Bis(4-nitrophenyl)-*N,N'*-di(4-(1,2,2-triphenylethenyl)phenyl)-1,4-phenylenediamine (TPPA-TPE-2NO₂, 3)**

TPPA-TPE-2NO₂ was synthesized through the Ullman coupling reaction. In a 250 mL round-bottom flask, a mixture of 2.1 g (6.0 mmol) of TPPA-2NO₂, 5.1 g (12.3 mmol) of TPE-Br, 1.6 g (24.0 mmol) of copper powder, 6.6 g (48.0 mmol) of K₂CO₃ and 0.9 g (3.3 mmol) of 18-crown-6 ether was dispersed in 25 mL of *o*-dichlorobenzene, and stirred under nitrogen atmosphere at 160 °C for 24 h. Then the inorganic salts and copper powder were filtered from the hot reaction mixture. The filtrate was poured into ethanol to precipitate a red crude product, which was purified by silica gel column chromatography (petroleum ether/ethyl acetate: 3/1) to yield 3.1 g of the desired TPPA-TPE-2NO₂ in 52 %. FTIR (KBr): 1310 cm⁻¹, 1580 cm⁻¹ (-NO₂ stretch). ¹H NMR (300 MHz, DMSO- d_6 , δ , ppm): 8.09 (d, $J = 9.2$ Hz, 4H), 7.25 – 7.12 (m, 5H), 7.09 – 6.96 (m, 5H), 6.83 (d, $J = 9.3$ Hz, 4H).

***N,N'*-Bis(4-aminophenyl)-*N,N'*-di(4-(1,2,2-triphenylethenyl)phenyl)-1,4-phenylenediamine (TPPA-TPE-2NH₂, 4)**

In a 250 mL round-bottom flask equipped with a stirring bar, 2.5 g (2.5 mmol) of TPPA-TPE-2NO₂ and 0.15 g of 10% Pd/C were dispersed in 40 mL of dioxane. After heating the suspension solution to reflux, 6.3 g of hydrazine monohydrate was dropwise added to the above mixture. After stirred at the reflux temperature for another 8 h, Pd/C was removed by immediate filtration, and the filtrate was cooled under a nitrogen flow to precipitate yellow powder. The powder was collected by filtration and dried under vacuum at 90 °C, yielding 1.7 g of the desired PDA-TPE-2NH₂ in 71 %. FTIR (KBr): 3375 cm⁻¹, 3458 cm⁻¹ (-NH₂ stretch). ¹H NMR (300 MHz, DMSO- d_6 , δ , ppm): 7.15 (t, $J = 7.5$ Hz, 4H, H_k), 7.13 – 7.04 (m, 14H, H_j+H_h+H_g), 6.98 (t, $J = 8.8$ Hz, 8H, H_i), 6.93 (d, $J = 7.5$ Hz, 4H, H_f), 6.78 (s, 4H, H_c), 6.75 (d, $J = 8.1$ Hz, 4H, H_e), 6.71 (d, $J = 8.2$ Hz, 4H, H_b), 6.58 – 6.49 (m, 8H, H_d+H_a), 5.04 (s, 4H, -NH₂). ¹³C NMR (75 MHz, DMSO- d_6 , δ , ppm): 147.18, 146.66, 144.10, 143.99, 143.80, 142.32, 140.98, 139.85, 135.32, 135.01, 131.85, 131.18, 128.33, 128.20, 126.88, 126.77, 126.73, 124.38, 119.05, 115.36.

Polymer synthesis (TPPA-TPE-PA, 5)

The novel polyamide TPPA-TPE-PA was synthesized from the as-prepared diamine TPPA-TPE-2NH₂ and dicarboxylic acid (CHDA) through a direct polycondensation (Scheme 1b).⁴⁸ 0.951 g (1 mmol) of TPPA-TPE-2NH₂, 0.172 g (1 mmol) of CHDA, 0.2 g of CaCl₂, 1 mL of TPP, 0.5 mL of Py and 2 mL of NMP were heated with stirring at 110 °C for 4 h. After cooling to room temperature, the resulting polymer solution was slowly poured into vigorously stirred ethanol to produce a fiber-like precipitate, which was collected by filtration, purified by Soxhlet extraction with water and ethanol, and then dried under vacuum at 80 °C. ¹H NMR (300 MHz, DMSO- d_6 , δ , ppm):

9.80 (s, 2H, amide), 7.54 (d, $J = 8.9$ Hz, 4H, H_a), 7.25 – 7.08 (m, 18H, H_k+H_j+H_h+H_g), 7.07 – 6.90 (m, 16H, H_i+H_f+H_b), 6.85 (s, 4H, H_c), 6.82 (d, $J = 8.7$ Hz, 4H, H_e), 6.67 (d, $J = 8.7$ Hz, 4H, H_d).

Measurements

Nuclear magnetic resonance (NMR) spectra were collected on a BRUKER-300 spectrometer using deuterated DMSO as a solvent. Fourier transform infrared (FTIR) spectra were recorded through a Bruker Vector 22 spectrometer in the range of 400-4000 cm⁻¹. Gel permeation chromatographic (GPC) analysis was carried out on a PL-GPV 220 instrument with DMF as an eluent at a flow rate of 1.0 mL/min, and was calibrated with polystyrene standards. Differential scanning calorimetric (DSC) analysis was performed on TA Q100 at a scanning rate of 10 °C/min in a nitrogen flow of 50 mL/min. Thermo gravimetric analysis (TGA) in the temperature range of 100-800 °C was obtained on the TA 2050, with a heating rate of 10 °C/min under nitrogen atmosphere. Electrochemical measurements were performed by a CHI 660e electrochemical workstation. Cyclic voltammetry (CV) tests were conducted in a common liquid cell with polymer film coated on an ITO glass as the working electrode, a platinum wire as an auxiliary electrode, an Ag/AgCl, KCl (sat.) as a reference electrode and 0.1 M TBAP in dried CH₃CN as the supporting electrolyte, respectively. UV-vis-NIR spectra were recorded by a Shimadzu UV 3101-PC spectrophotometer. Photoluminescence (PL) spectra were determined with an Edinburgh FLS920 fluorescence spectrophotometer. The spectroelectrochemical cell was composed of a 1 cm cuvette with a three-electrode system similar to the CV tests.

Results and discussion

Synthesis and characterization of the diamine and polyamide

A novel electroactive/AIE-active diamine with TPPA and TPE was synthesized by a multi-step procedure as depicted in Scheme 1a. TPE-Br 1 was synthesized by McMurry reaction between 4-bromobenzophenone and benzophenone. TPPA-2NO₂ 2 was obtained from a nucleophilic substitution reaction of *p*-phenylenediamine and 4-fluoronitrobenzene under trimethylamine assistance. Then, TPPA-TPE-2NO₂ 3 was successfully synthesized by Ullman reaction of TPE-Br and TPPA-2NO₂. Subsequent reduction of TPPA-TPE-2NO₂ by means of Pd/C and hydrazine gave the target diamine TPPA-TPE-2NH₂ 4. The chemical structures of these four monomers were identified by FTIR and NMR analysis. The FTIR spectra of TPPA-TPE-2NH₂ shows the characteristic stretching absorption pairs of amino groups at 3375 cm⁻¹ and 3458 cm⁻¹ (Fig. S1). The ¹H NMR together with its COSY spectra and ¹³C NMR spectrum of TPPA-TPE-2NH₂ are illustrated in Fig. S2 and Fig. S3, from which it is observed that all the resonances signals are well assigned to the protons of the molecular structure, indicating the successful synthesis of the target diamine. After synthesizing the pure TPPA-TPE-2NH₂, the subtly designed luminophor with TPPA and TPE units could be readily incorporated into the polyamide backbones by a conventional

polymerization (Scheme 1b). The structure of the resulting polyamide TPPA-TPE-PA 5 were also confirmed by FTIR and NMR techniques. As shown in Fig. S4, the FTIR spectrum revealed characteristic amide stretching absorption bands at 3310 cm^{-1} (N-H) and 1662 cm^{-1} (C=O). The ^1H NMR spectrum of TPPA-TPE-PA was illustrated in Fig. S5, showing proton signals corresponding well to the hydrogen atoms in a polyamide repeat unit. Thus, all the above results demonstrate that the novel polyamide with electroactive TPPA and AIE-active TPE units was successfully synthesized.

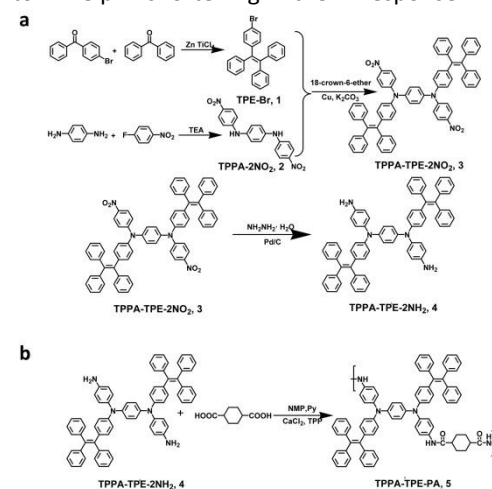
To further reveal the inherent physical properties of TPPA-TPE-PA, its molecular weight, inherent viscosity, solubility behavior and thermal properties were systematically studied. The number-average molecular weights and polydispersity of TPPA-TPE-PA were tested to be 41200 and 1.36, respectively. The inherent viscosity was measured to be 1.09, further indicating the high molecular, which is beneficial for the thermal and mechanical properties. The solubility was evaluated at 10% w/v concentration in various organic solvents. As listed in Table S1, TPPA-TPE-PA exhibited excellent solubility, demonstrating that the polyamide film could be facilely fabricated by competitive solution casting, a major advantage for practical application. Additionally, the thermal properties of TPPA-TPE-PA were investigated by TGA and DSC (Fig. S6). TPPA-TPE-PA revealed high thermal stability with 10 % weight loss happened at $467\text{ }^\circ\text{C}$ and the glass transition temperature was found up to $244\text{ }^\circ\text{C}$.

Electrochemical and electrochromic properties

The electrochemical analyses of TPPA-TPE-PA by cyclic voltammetry (CV) were conducted in a three electrode system with a TPPA-TPE-PA thin film coated on an ITO substrate as the working electrode, an Ag/AgCl as a reference electrode, a platinum wire as a counter electrode and 0.1 M TBAP/ CH_3CN as the supporting electrolyte. The CV curves revealed two quasi-reversible redox couples at $0.74/0.39\text{ V}$ and $1.12/0.75\text{ V}$, respectively. After 100 continuous cyclic scans, the TPPA-TPE-PA thin film maintained a good CV reversibility with only a small decrease of peak current (Fig. 2a). Remarkably, the first redox process from 0.00 V to 0.70 V exhibited a much more stable electrochemical behavior due to the low oxidation potentials ($E_{\text{onset}} = 0.40\text{ V}$) and the highly conjugated TPPA structure (Fig. 2b). The superior CV reversibility in continuous 500 cyclic scans demonstrates that the first oxidation stage possesses a more valuable application potential, which could be utilized as a promising electro-switching modulator.

During the CV scanning process, the TPPA-TPE-PA thin film revealed obvious two-stage color changes. Thus spectroelectrochemical experiments were employed to further evaluate the optical properties of the EC film. For this investigation, the polymer film was monitored in situ by a UV-vis spectrophotometer under the potential control of an electrochemistry workstation. As shown in Fig. 2c, upon oxidation (steadily increasing potentials from 0.00 V to 0.70 V), the intensity of the absorption band at 342 nm in the neutral

state gradually decreased. Meanwhile, two new bands at 421 nm in the visible region and 1154 nm in the near-infrared region appeared, corresponding to the formation of the monocation radical of TPPA-TPE-PA. The near-infrared absorption was ascribed to an inter-valence charge transfer effect.⁴² With the applied potentials increased from 0.70 V to 1.10 V , the monocation radical of TPPA-TPE-PA was further oxidized to the dication radical, accompanied by a decrease of the absorption bands at 421 nm and 1154 nm and the emergence of a new absorption band at 858 nm . The series of absorption spectra changes are well consistent with the distinguished color changes of the TPPA-TPE-PA film. The polymer film switched its apparent color from near colorless in the neutral state to green-yellow in the first oxidation state and then to light blue in the second oxidation state. Moreover, kinetic studies were performed to estimate the EC switching stability and response time. The EC film of TPPA-TPE-PA in the first redox state exhibited stable switching properties over 500 cycles (Fig. S7). The excellent stability compared with the PA containing diphenylamine-TPE unit could be attributed to the low oxidation potential and increased resonance stability of the highly conjugated TPPA unit.³⁶ As for the second redox state, the absorbance decreased gradually after continuous 300 cycles, which could be attributed to the side reactions caused by the applied high voltage. It is worth noting that TPPA-TPE-PA displays a very fast response rate, showing the coloration/bleaching time $1.3/0.5\text{ s}$ at 421 nm , $1.5/0.8\text{ s}$ at 1154 nm and $1.2/0.6\text{ s}$ at 858 nm . The intrinsic switching time is much shorter than most of the EC polymers (even hybrid materials), and is the shortest value to our knowledge for the TPA-based EC polymers.^{30,43} The fast response benefits from the incorporation of the highly twisted TPPA and TPE units, leading to a loose polymer chain packing and an efficiently accelerated ion-diffusion in the polymer film (Fig. S7). Besides, in comparison with mono-TPA unit, the highly conjugated TPPA can enhance the intra-molecular charge mobility ability to help shortening the response time as well.



Scheme 1 Synthetic route of the diamine TPPA-TPE-2NH₂ (a) and the polyamide TPPA-TPE-PA (b).

Fluorescence and EFC properties

The interesting photophysical properties of the polymer were further investigated regarding the fluorescence and EFC properties. The absorption spectra of TPPA-TPE-PA exhibited

similar maximum absorption peaks (316 and 318 nm) in NMP solution and drop-cast film states (Fig. S8). In comparison, the fluorescence spectra showed a huge difference between solution and solid state. TPPA-TPE-PA in NMP solution

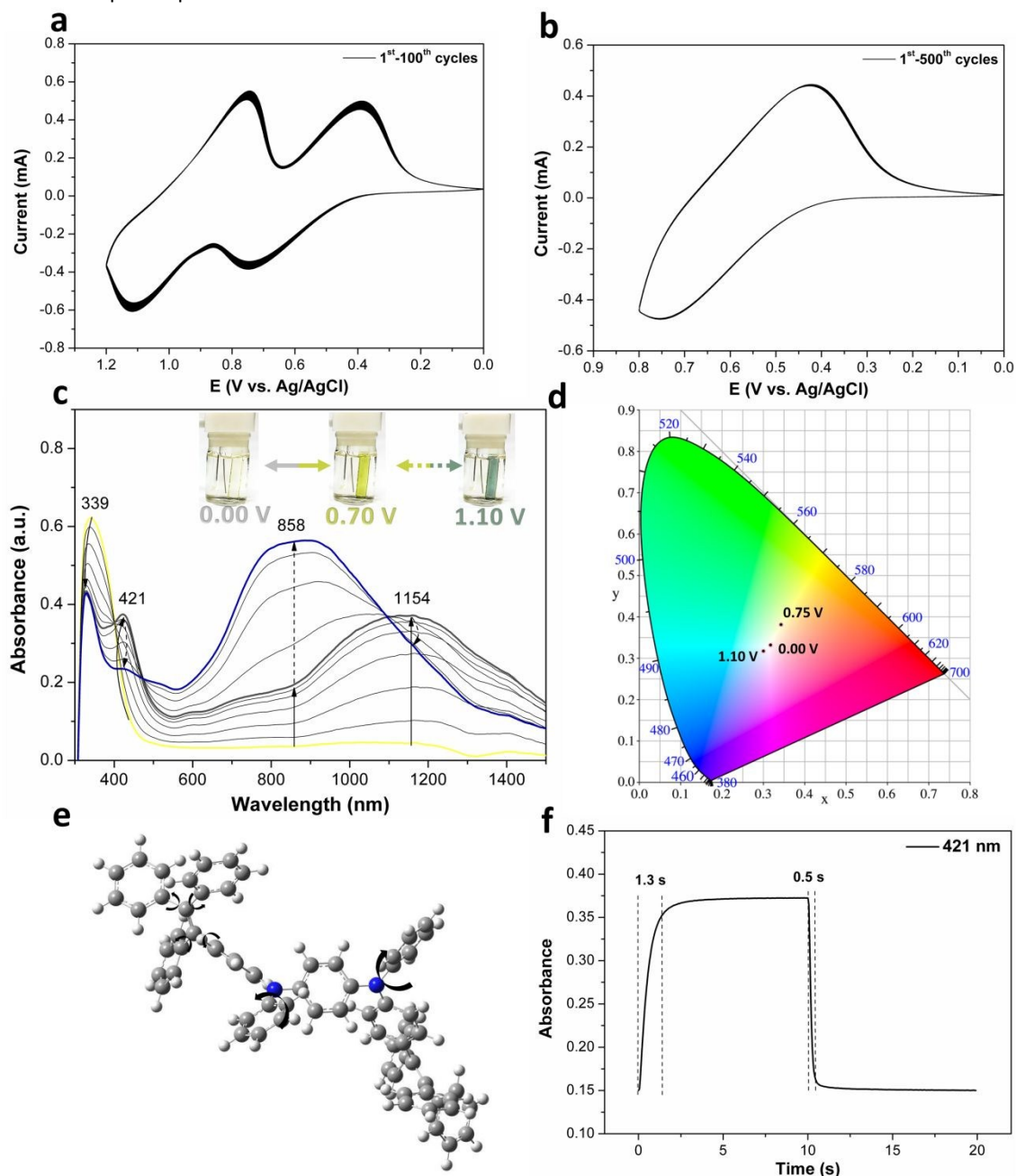


Fig. 2 (a) CV diagram of TPPA-TPE-PA from 0.00 V to 1.20 V. (b) CV diagram from 0.00 V to 0.80 V for the first redox process. (c) Absorbance spectra of TPPA-TPE-PA thin film electrode in 0.1 M TBAP/CH₃CN at different applied potentials from 0.00 V to 1.10 V. (d) CIE chromaticity at different potentials (0.00 V Xy: 97.56, 0.3053, 0.3139; 0.80 V Xy: 44.77, 0.3131, 0.3172). (e) Twist structure of TPPA-TPE. (f) EC switching time of TPPA-TPE-PA thin film electrode between 0.00 V and 0.07 V.

revealed rather weak emission intensity, whereas the fluorescence of TPPA-TPE-PA in the solid state was greatly enhanced, demonstrating a pronounced AIE characteristic. To further investigate the AIE effect, we tested the fluorescence of TPPA-TPE-PA in NMP-water mixtures containing different water fractions. TPPA-TPE-PA express a weak fluorescence in

the pure NMP solution. Gradually increasing the water fraction from 0% to 90% in the NMP-water mixtures enhanced the fluorescence emission accordingly, which can be visually observed in the inset images of Fig. 3a. The active intramolecular motion of TPPA and TPE in NMP consumes the exciton energy through nonradiative relaxation channel, while

the aggregation of TPPA-TPE-PA in NMP-water mixtures activates the RIR process, resulting in the significant fluorescence enhancement.¹⁹

Furthermore, when the TPPA-TPE moiety was oxidized to its cation radical, the combined effect of absorption band shift, structural planarization and electron effect changing electron donating to electron withdrawing could effectively quench the strong fluorescence of TPPA-TPE-PA. Therefore, the switchable fluorescence properties in response to electrochemical redox were further investigated by recording the fluorescence spectra of TPPA-TPE-PA at different applied potentials. As depicted in Fig. 3c, the AIE-active TPPA-TPE-PA film emits

bright green-yellow light, which can be quenched to dark when applying the positive potentials from 0.00 V to 0.80 V. In this testing process, the fluorescence intensity at 532 nm dramatically decreased and the fluorescence on/off contrast between neutral fluorescent state and oxidized non-fluorescent state reached up to 252 (Fig. 3d). With the applications of the reverse potential, the fluorescence recovered, indicating a reversible fluorescence modulation. The systematical investigation of fluorescence switching behavior is discussed below.

EFC switching performances

The response of the fluorescence switching was examined by

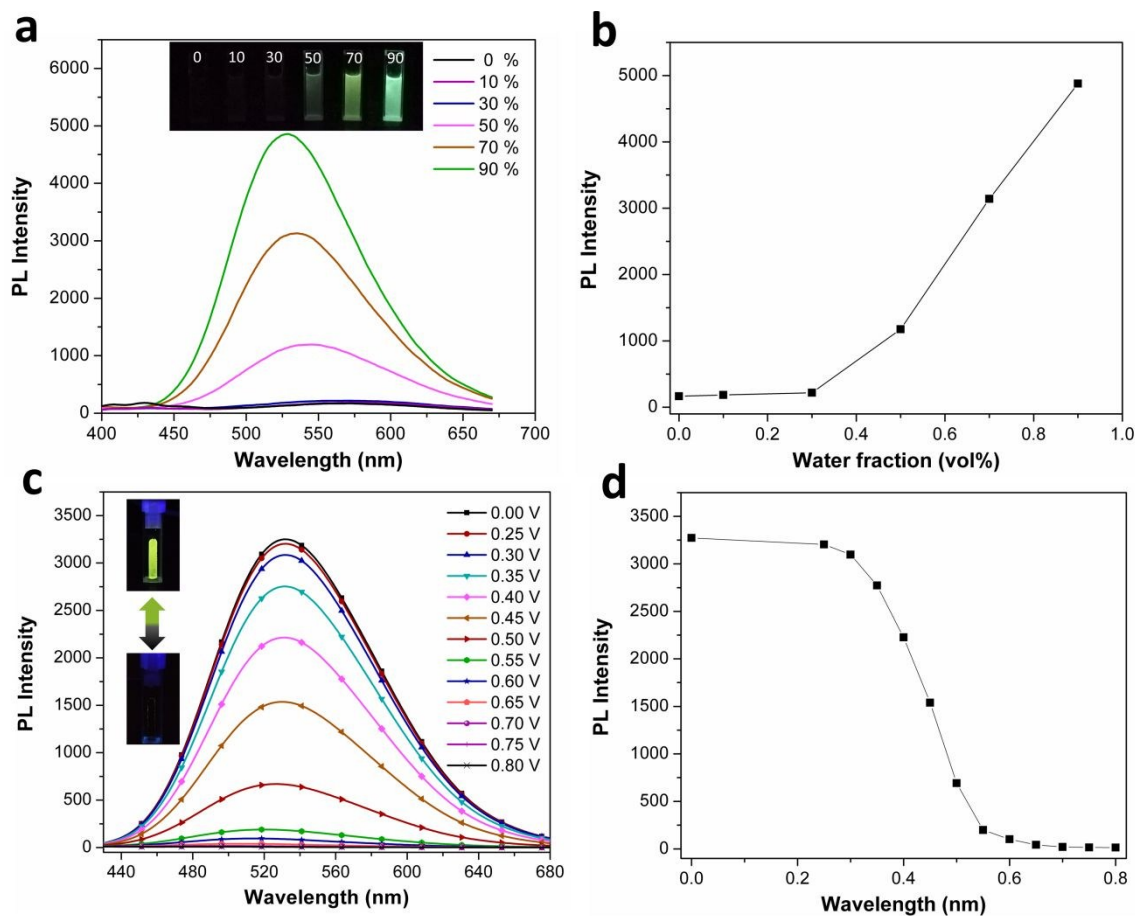


Fig. 3 (a) PL spectra of TPPA-TPE-PA in NMP-water mixtures with different water contents (inset: fluorescence images in NMP-water mixtures). (b) Increase of PL intensity with the increasing water fraction of NMP-water mixtures. (c) PL spectra changes of TPPA-TPE-PA film at different applied potentials from 0.00 V to 0.80 V. (d) Decrease of PL intensity with the applied potentials increased from 0.00 V to 0.80 V.

monitoring the fluorescence emission changes when applying stepping potentials. To realize the optimized fluorescence switching, the influence of the applied potentials was investigated by changing the oxidation potentials from 0.30 V to 0.80 V. As shown in Fig. 4a, with the oxidation potentials increased (at a duration time of 10 s), the fluorescence intensity is quenched to a lower value together with a faster quenching speed, resulting from the larger potential difference. During the fluorescence recovering process,

applying 0.80 V potential led to a slower response speed and lower on/off contrast compared with 0.70 V. This phenomenon may be ascribed to the decrease of the absorption band in the range of 420-500 nm and more ions getting trapped in the polymer film. Therefore, repetitive applying voltage pulses between 0.00 V and 0.70 V was selected as the optimal condition to switch the fluorescence on/off states. Additionally, the fluorescence switching behavior at different duration time was also studied. When

progressively increasing the duration time from 10 s to 360 s, the fluorescence on/off contrast increased on account of the more completed redox reaction in the longer duration time. Notably, compared with previously reported EFC materials,^{7,15,16} which usually showed a decrease of the fluorescence contrast upon shortening of the duration time, TPPA-TPE-PA largely maintained its high fluorescence on/off contrast with the duration time shortened. This feature is benefiting from the faster response kinetics, and could enable a high fluorescence contrast under a short duration time. To circumvent the inherent contradiction between switching time and fluorescence contrast, the long-term stability was finally

measured at the duration time of 20 s. As shown in Fig. 4c, the EFC switching of TPPA-TPE-PA exhibited superb stability with only slight delay in continuous 10000 s (500 cycles). In view of the solution switching condition used here, it is feasible to expect that the even improved switching stability could be attained on optimization of the EFC devices (packaging the device, introduction of counter layer for charge balance and so on). The excellent switching stability in comparison with mono-TPA-based materials could also attributed to the excellent electrochemical stability of TPPA structure. The EFC switching time calculated at 90% of full modulation was 0.7 s and 2.1 s for fluorescence

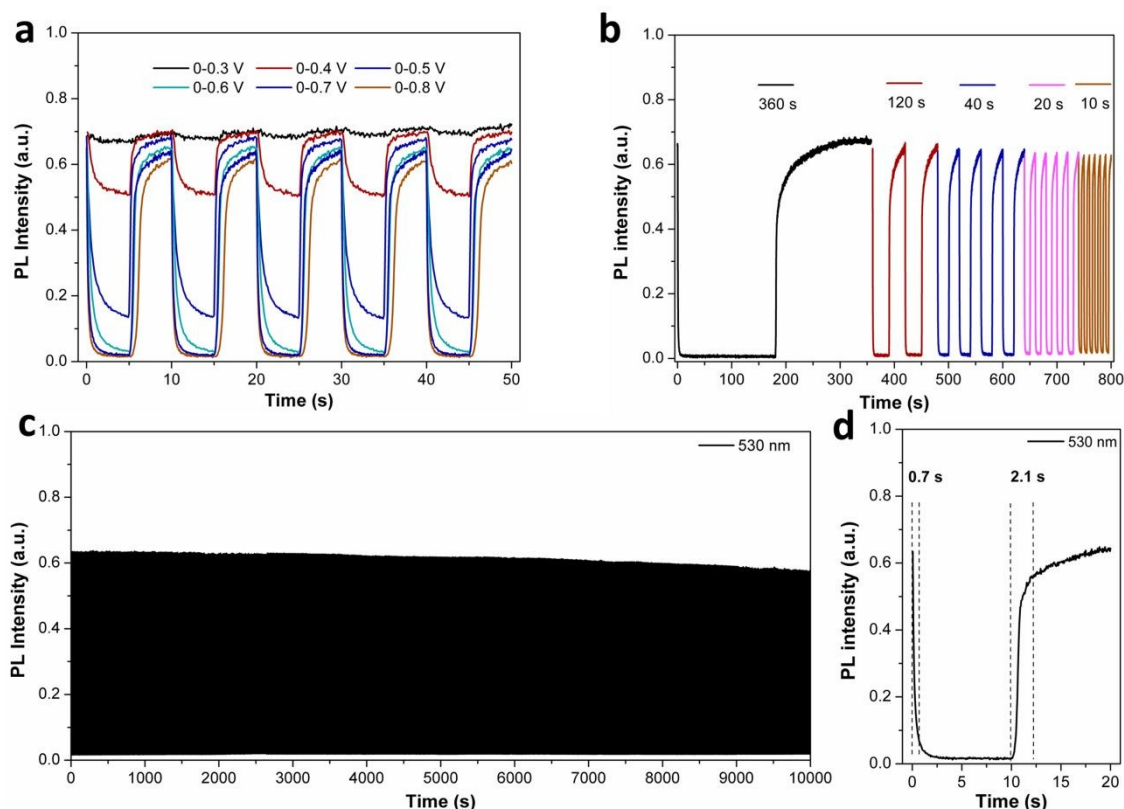


Fig. 4 (a) Fluorescence switching response of TPPA-TPE-PA at different double potential steps from 0.00 V to 0.30 V, 0.40 V, 0.50 V, 0.60 V, 0.70 V and 0.80 V. (b) Fluorescence switching response under applied potentials between 0 V and 0.7 V with different step cycle time from 360 s to 10 s. (c) Long-term fluorescence switching at the step cycle time of 20 s for continuous 10000 s. (d) Response time of the fluorescence switching at the step cycle time of 20 s: 0.7 s and 2.1 s for fluorescence off and on processes estimated at 90% of the full modulation.

quenching and lighting processes, respectively. The excellent fluorescence on/off response speed can be attributed to the synergistic effect of the introduction of highly twisted TPE and the conjugated TPPA units, facilitating the transport of electrolyte ions and enhancing intra-molecular charge mobility. In comparison to the EC process, the relatively longer response time of EFC switching may be ascribed to the more sensitive characteristic of fluorescence. Furthermore, thanks to the AIE-activity and fast response kinetics of TPPA-TPE-PA,

the fluorescence on/off contrast was found up to 82 at the duration time of 20 s. Even if only partial fluorescence was recovered, the value is still much higher than those reported in the previous studies.^{14,16,17} Thus, a EFC polymer with highly integrated performances comprising superb cycling stability, fast response speed, high fluorescence on/off contrast and facile solution-processability was effectively realized, paving a way for the smart applications in the future.

Conclusion

In summary, a molecular-design concept synergistically introducing TPE and TPPA was used to prepare a novel electroactive and AIE-active polymer. In addition to the excellent thermal and solubility properties, the resulting polyamide TPPA-TPE-PA also exhibited high solid-state fluorescence and outstanding electrochemistry stability. EC process of TPPA-TPE-PA showed two-stage color changes (colorless to green to blue), while EFC process stably revealed a switching between bright fluorescence and quenching dark. Remarkably, TPPA-TPE-PA achieved highly integrated EC and EFC performances comprising fast intrinsic response speed, high optical contrast up to 252 and splendid long-term stability in continuous 10000 s by the synergistic effect of TPE and TPPA moieties, which opens up a new pathway for designing high-performance switchable optical materials and enables widespread applications in multifunctional optoelectronic devices and sensors.

Conflicts of interest

There are no conflicts to declare.

Acknowledgements

References

- 1 K. Stratford, O. Henrich, J. S. Lintuvuori, M. E. Cates and D. Marenduzzo, *Nat. Commun.*, 2014, **5**, 3954.
- 2 O. Sato, *Nat. Chem.*, 2016, **8**, 644.
- 3 R. J. Mortimer, A. L. Dyer and J. R. Reynolds, *Displays*, 2006, **27**, 2.
- 4 D. Kim, J. E. Kwon and S. Y. Park, *Adv. Funct. Mater.*, 2018, **28**, 1706213.
- 5 Z. Zhou, Y. Yu, N. Sun, H. Möhwald, P. Gu, L. Wang, W. Zhang, T. A. F. König, A. Fery and G. Zhang, *ACS Appl. Mater. Interfaces*, 2017, **9**, 35244.
- 6 P. Audebert and F. Miomandre, *Chem. Sci.*, 2013, **4**, 575.
- 7 J. Sun, Y. Chen and Z. Liang, *Adv. Funct. Mater.*, 2016, **26**, 2783.
- 8 H. Al-Kutubi, H. R. Zafarani, L. Rassaei and K. Mathwig, *Eur. Polym. J.*, 2016, **83**, 478.
- 9 A. Beneduci, S. Cospito, M. La Deda, L. Veltri and G. Chidichimo, *Nat. Commun.*, 2014, **5**, 3105.
- 10 X. Wang, W. Li, W. Li, C. Gu, H. Zheng, Y. Wang, Y.-M. Zhang, M. Li and S. X.-A. Zhang, *Chem. Commun.*, 2017, **53**, 11209.
- 11 K. Kanazawa, K. Nakamura and N. Kobayashi, *Sol. Energy Mater. Sol. Cells*, 2016, **145**, 42.
- 12 Q. Ma, H. Zhang, J. Chen, S. Dong and Y. Fang, *Chem. Commun.*, 2019, **55**, 644.
- 13 A. N. Woodward, J. M. Kolesar, S. R. Hall, N.-A. Saleh, D. S. Jones and M. G. Walter, *J. Am. Chem. Soc.*, 2017, **139**, 8467.
- 14 J.-T. Wu, H.-T. Lin and G.-S. Liou, *ACS Appl. Mater. Interfaces*, 2019, **11**, 14902. DOI: 10.1039/C9TC02001B
- 15 S. Seo, Y. Kim, J. You, B. D. Sarwade, P. P. Wadgaonkar, S. K. Menon and A. S. More, *Macromol. Rapid Commun.*, 2011, **32**, 637.
- 16 J.-H. Wu and G.-S. Liou, *Adv. Funct. Mater.*, 2014, **24**, 6422.
- 17 N. Sun, S. Meng, D. Chao, Z. Zhou, Y. Du, D. Wang, X. Zhao, H. Zhou and C. Chen, *Polym. Chem.*, 2016, **7**, 6055.
- 18 C.-P. Kuo, C.-N. Chuang, C.-L. Chang, M.-k. Leung, H.-Y. Lian and K. C.-W. Wu, *J. Mater. Chem. C*, 2013, **1**, 2121.
- 19 J. Mei, N. L. C. Leung, R. T. K. Kwok, J. W. Y. Lam and B. Z. Tang, *Chem. Rev.*, 2015, **115**, 11718.
- 20 J. Mei, Y. Hong, J. W. Y. Lam, A. Qin, Y. Tang and B. Z. Tang, *Adv. Mater.*, 2014, **26**, 5429.
- 21 X. Fang, Y. Zhang, K. Chang, Z. Liu, X. Su, H. Chen, S. X.-A. Zhang, Y. Liu and C. Wu, *Chem. Mater.*, 2016, **28**, 6628.
- 22 S. Abraham, S. Mangalath, D. Sasikumar and J. Joseph, *Chem. Mater.*, 2017, **29**, 9877.
- 23 Y. Bao, E. Guégain, V. Nicolas and J. Nicolas, *Chem. Commun.*, 2017, **53**, 4489.
- 24 X. Liu and G. Liang, *Chem. Commun.*, 2017, **53**, 1037.
- 25 R. Rathore, S. V. Lindeman, A. S. Kumar and J. K. Kochi, *J. Am. Chem. Soc.*, 1998, **120**, 6931.
- 26 Y. Shirota, *J. Mater. Chem.*, 2005, **15**, 75.
- 27 G. Zhang, H. Bala, Y. Cheng, D. Shi, X. Lv, Q. Yu and P. Wang, *Chem. Commun.*, 2009, **16**, 2198.
- 28 P. Cias, C. Slugovc and G. Gescheidt, *J. Phys. Chem. A*, 2011, **115**, 14519.
- 29 H.-J. Yen and G.-S. Liou, *Polym. Chem.*, 2012, **3**, 255.
- 30 Y. Yan, N. Sun, X. Jia, X. Liu, C. Wang and D. Chao, *Polymer*, 2018, **134**, 1.
- 31 K. Su, N. Sun, X. Tian, S. Guo, Z. Yan, D. Wang, H. Zhou, X. Zhao and C. Chen, *J. Mater. Chem. C*, 2019, **16**, 4644.
- 32 N. Sun, S. Meng, Z. Zhou, J. Yao, Y. Du, D. Wang, X. Zhao, H. Zhou and C. Chen, *RSC Adv.*, 2016, **6**, 66288.
- 33 N. Sun, X. Tian, L. Hong, K. Su, Z. Zhou, S. Jin, D. Wang, X. Zhao, H. Zhou and C. Chen, *Electrochim. Acta*, 2018, **284**, 655.
- 34 N. Sun, Z. Zhou, S. Meng, D. Chao, X. Chu, X. Zhao, D. Wang, H. Zhou and C. Chen, *Dyes Pigm.*, 2017, **141**, 356.
- 35 L. Hao, W. Wang, H. Niu and Y. Zhou, *Electrochim. Acta*, 2017, **246**, 259.
- 36 J. Sun, X. Lv, P. Wang, Y. Zhang, Y. Dai, Q. Wu, M. Ouyang and C. Zhang, *J. Mater. Chem. C*, 2014, **2**, 5365.
- 37 M. Ouyang, G. Wang and C. Zhang, *Electrochim. Acta*, 2011, **56**, 4645.
- 38 N. Sun, K. Su, Z. Zhou, Y. Yu, X. Tian, D. Wang, X. Zhao, H. Zhou and C. Chen, *ACS Appl. Mater. Interfaces*, 2018, **10**, 16105.
- 39 S.-Y. Chen, Y.-W. Chiu and G.-S. Liou, *Nanoscale*, 2019, **11**, 8597.
- 40 H.-T. Lin, C.-L. Huang and G.-S. Liou, *ACS Appl. Mater. Interfaces*, 2019, **11**, 11684.
- 41 H.-J. Yen and G.-S. Liou, *Chem. Mater.*, 2009, **21**, 4062.

Journal Name

ARTICLE

- 42 H. J. Yen, C. J. Chen and G. S. Liou, *Adv. Funct. Mater.*, 2013, **23**, 5307.
- 43 N. Sun, S. Meng, Z. Zhou, D. Chao, Y. Yu, K. Su, D. Wang, X. Zhao, H. Zhou and C. Chen, *Electrochim. Acta*, 2017, **256**, 119.
- 44 C. Lambert and G. Nöll, *J. Am. Chem. Soc.*, 1999, **121**, 8434.
- 45 V. K. Thakur, G. Ding, J. Ma, P. S. Lee and X. Lu, *Adv. Mater.*, 2012, **24**, 4071.
- 46 X.-F. Duan, J. Zeng, J.-W. Lü and Z.-B. Zhang, *J. Org. Chem.*, 2006, **71**, 9873.
- 47 I. Różalska, P. Kułyk and I. Kulszewicz-Bajer, *New J. Chem.*, 2004, **28**, 1235.
- 48 N. Yamazaki, F. Higashi and J. Kawabata, *J. Polym. Sci. Polym. Chem. Ed.*, 1974, **12**, 2149.

View Article Online
DOI: 10.1039/C9TC02001B

Table of Contents

Based on the design concept by combining highly conjugated p-phenylenediamine and AIE-active tetraphenylethylene, a novel electroactive/fluorescent polymer was successfully synthesized. The resulting polymer exhibited highly integrated electrochromic /electrofluorochromic performances including high solid-state fluorescence, highly stable electrochemistry over 500 cycles, high fluorescence on/off contrast of 252, long-term switching stability over 10000 s and fast EC/EFC response speed.

